第 29 卷第 11 期 无 机 化 学 学 报 Vol.29 No.11
2013 年 11 月 CHINESE JOURNAL OF INORGANIC CHEMISTRY 2405-2414

对甲醛苯甲酸构筑的 Cu(Ⅱ)配合物:合成,结构及磁性质

戚金丽 郑岳青* 许 伟
(宁波大学应用固体化学研究中心,宁波 315211)

摘要:采用室温溶液法合成两例新 Cu(Ⅱ)配合物[Cu(phen)(H_2O)(fba)(ClO_4)]·H_2O (**1**),$^1_\infty$[Cu(bpy)(H_2O)(fba)$_2$] (**2**)(Hfba=对甲醛苯甲酸,phen=1,10-邻菲啰啉,bpy=2,2′-联吡啶),通过 X-射线单晶衍射、X-射线粉末衍射、红外光谱、热重分析和元素分析方法对其表征。化合物 **1**、**2** 分别为单核、一维链结构,均通过非共价键作用形成三维超分子构造。**1** 和 **2** 的变温磁化率研究表明:**1** 中金属离子在 300~7 和 7~2 K 温度区间分别显示铁磁性和反铁磁性耦合,**2** 中金属离子在测试温度范围内为反铁磁性耦合。

关键词:合成;晶体结构;非共价键作用;磁性质
中图分类号:O614.121 **文献标识码**:A **文章编号**:1001-4861(2013)11-2405-10
DOI:10.3969/j.issn.1001-4861.2013.00.380

Use of *p*-Formylbenzoate to Construct two Copper(Ⅱ) Complexes: Syntheses, Crystal Structures and Magnetic Properties

QI Jin-Li ZHENG Yue-Qing* XU Wei
(*Center of Applied Solid State Chemistry Research, Ningbo University, Ningbo, Zhejiang* 315211, *China*)

Abstract: Two new Cu(Ⅱ) complexes, [Cu(phen)(H_2O)(fba)(ClO_4)]·H_2O (**1**) and $^1_\infty$[Cu(bpy)(H_2O)(fba)$_2$] (**2**) (phen=phenanthroline, bpy=2,2′-bipyridine Hfba=p-formylbenzoic acid) were synthesized by solution-based method and characterized by single-crystal, powder X-ray diffraction methods, IR spectroscopy, TG-DTA analyses, elemental analyses, and magnetic measurements. Compound **1** is a mononuclear structure crystallizing in the space group $P\bar{1}$ and **2** shows a 1D chain structure which belongs to the space group *Pbca*. Through non-covalent interactions the complex molecules are assembled into 3D supramolecular network structures. The variable temperature magnetic measurements of **1** shows a weak ferromagnetic and antiferromagnetic behavior in the range of 300~7 and 7~2 K, respectively, while the **2**′s suggests very weak ferromagnetic interactions between Cu(Ⅱ) ions in the experimental temperature range. CCDC: 912745, **1**; CCDC: 912746, **2**.

Key words: syntheses; crystal structure; non-covalent interactions; magnetic properties

0 Introduction

Supramolecular chemistry and crystal engineering have attracted increasing attention due to their intriguing network architectures and structural topologies, as well as their potential applications in catalyses, separations, gas storages, optical properties, magnetic properties, ect.[1-4]. As we all know, non-covalent interactions can make contribution to the construction of supramolecular networks from simple units [5-7]. The relatively strong interactions like O–H···O hydrogen bonds are extensive organizing force in

收稿日期:2013-04-28。收修改稿日期:2013-06-28。
应用非线性科学与技术浙江省重中之重学科开放基金(No.xkzl2006),宁波大学王宽诚幸福基金资助项目。
*通讯联系人。E-mail:yqzhengmc@163.com

the assembling of supramolecules, and the individually weak interactions such as $\pi\cdots\pi$ stacking, close packing interactions, C–H···O hydrogen bonds are common now, however, those non-covalent interactions together play an important role in the formation of 3D supramolecular network structures are relatively less reported at present[8].

The carboxylic acids containing benzene-core are rich in coordination modes and extensively used in the synthesis of complexes function as hydrogen-bond acceptors as well as donors[9-11]. For *p*-formylbenzoic acid (Hfba), the O atom on formal group can also function as hydrogen-bond acceptor[12-13]. Of the many compounds investigated, an effective approach to obtain a low dimension complex is incorporating a terminal ligand such as phen and bpy which can also contribute themselves to the formation of supramolecular systems via $\pi\cdots\pi$ stacking interactions[14-16]. For achieving low dimension complexes and studying how the non-covalent interactions function in the assembly from simple units into 3D supramolecular structures, we choose monocarboxylic acid Hfba, terminal ligand phen and bpy as ligands.

In the past contribution, we had prepared two Cu(Ⅱ) complexes using *p*-formylbenzoic acid[17-18]. To extending our work, we synthesized another two new Cu(Ⅱ) complexes, and studied the relevant magnetic properties and how the non-covalent interactions work in the construction of supramolecules.

1 Experimental

1.1 Materials and measurements

All chemicals purchased were of analytical reagent and used without further purification. Powder X-ray diffraction (PXRD) measurements were carried out with a Bruker D8 Focus X-ray diffractometer using a Cu target (λ=0.154 056 nm) and a Ni filter at room temperature with the range of 2θ between 5° and 50°. Single crystal data were collected with a Rigaku R-Axis Rapid IP X-ray diffractometer using a Mo target (λ=0.071 073 nm). The infrared spectra were recorded in the range 4000~400 cm^{-1} using KBr pellets with an FTIR 8900 spectrometer. Thermogravimetric measurements were performed under a flow of nitrogen gas from room temperature to 800 °C at a heating rate of 10 ℃·min^{-1} by using a Seiko TG/DTA 6300 apparatus. The C, N and H microanalyses were performed with a Perkin-Elmer 2400 elemental analyzer. The temperature-dependent magnetic susceptibilities were determined with a Quantum Design SQUID magnetometer (Quantum Design Model MPMS-7) in the temperature range 2~300 K.

1.2 Synthesis of [Cu(phen)(H_2O)(fba)(ClO_4)]·H_2O (1)

0.075 g (0.5 mmol) Hfba and 0.5 mL 1 mol·L^{-1} NaOH were added to a mixed ethanolic aqueous solution (5.0 mL+5.0 mL) giving a yellow solution. 0.186 g (0.5 mmol) $Cu(ClO_4)_2\cdot 6H_2O$ was dissolved in another mixed ethanolic aqueous solution as before which was then added to the yellow solution producing blue precipitate. To the resulting suspension was added an ethanolic aqueous solution of 0.098 g (0.5 mmol) phen·H_2O, then the mixture being dark in color. After stirring, undissolved solid (0.177 g) was filtered out, and the dark blue filtrate (pH=5.40) was allowed to stand at room temperature. Blue plate-shaped crystals of **1** emerged after 1 d, and no deterioration was observed. PXRD measurements and elemental analyses confirmed that the undissolved solid and the blue crystals are the same phase. Finally, 0.197 g product was collected (yield: ca. 73% based on the initial $Cu(ClO_4)_2\cdot 6H_2O$ input). Anal. Calcd. for $C_{20}H_{17}ClCuN_2O_9$ (%): C, 45.45; H, 3.19; N, 5.32. Found (%): C, 45.67; H, 3.04; N, 5.01. IR data (cm^{-1}, KBr): 3 442(s), 2 835(w), 2 725(w), 1 697(m), 1 635(w), 1 587(m), 1 541(m), 1 517(m), 1 423(m), 1 398(s), 1 202(m), 1 120(s), 1 081(s), 842(m), 806(m), 770(m), 719(m), 637(m).

1.3 Synthesis of $^1_\infty$[Cu(bpy)(H_2O)($fba)_2$] (2)

1 mL (1 mol·L^{-1}) NaOH was added to a solution of 0.085 g (0.5 mmol) $CuCl_2\cdot 2H_2O$ giving blue precipitate, Cl^- anions were removed by centrifugation. 5.0 mL H_2O and 5.0 mL EtOH were added to the blue precipitate. Soon afterwards, the blue suspension above and another aqueous ethanol solution of 0.078 g

(0.5 mmol) bpy were added successively to an aqueous ethanol suspension of 0.150 g (1.0 mmol) Hfba. The resulting blue solution (pH =5.02) was allowed to evaporate at room temperature. After several days, yielded blue cluster-shaped substance which was removed through filtering and then the mother liquid was sat aside. A period of time later, the blue block-shaped crystals were obtained (yield: 48% based on the initial $CuCl_2 \cdot 2H_2O$ input) and no deterioration was observed. The phase purity of the product was checked according to elemental analysis and powder X-ray pattern compared with the simulated PXRD based on the single crystal data. Anal. Calc. for $C_{26}H_{20}CuN_2O_7$(%): C, 58.34; H, 3.59; N, 5.36. Found (%): C, 58.26; H, 3.76; N, 5.23. IR spectrum data (cm^{-1}, KBr): 3 487(w), 3 318(w), 3 034 (w), 2 835(w), 2 725(w), 1 696(s), 1 597(vs), 1 558(s), 1 497(m), 1 451(m), 1 393(s), 1 203(s), 1 032(w), 806 (s), 770(vs), 731(m).

1.4 X-ray crystallography

Single crystal diffraction data were collected at 298 K on a Rigaku R-Axis Rapid IP X-ray diffractometer with graphite-monochromated Mo $K\alpha$ radiation (λ=0.071 073 nm). In the range of 3.08°<θ<27.44° for 1 (3.16°<θ<27.48° for **2**), a total of 10 107 reflections were collected (38 872 for **2**), of which 4638 were unique with R_{int}=0.032 9 (5 140 for **2**, R_{int}=0.109 1), 3 208 were observed with $I>2\sigma(I)$ (4 939 for **2**). The structures were solved by direct method using SHELXS-97 program[19]. All non-hydrogen atoms were located with successive difference Fourier syntheses and refined by full-matrix least-squares methods on F^2 of SHELX-97 program[20]. The hydrogen atoms from *p*-formylbenzoate ions were located in calculated positions assigned a fixed isotropic displacement parameter at 1.2 times the equivalent isotropic U of the atoms to which they were attached. The hydrogen atoms of water molecules were placed in difference Fourier map. The key crystallographic information is summarized in Table 1, the main data of bond distances and bond angles are given in Table 2, and H-bonding parameters are showed in Table 3.

CCDC: 912745, **1**; 912746, **2**.

Table 1　Crystal data and refinement details for 1 and 2

Complex	**1**	**2**
Empirical formula	$C_{20}H_{15}ClCuN_2O_9$	$C_{26}H_{20}CuN_2O_7$
Formula weight	528.36	535.98
Crystal habit, color	Blue, block	Blue, chunk
Crystal system	Triclinc	Orthorhombic
Space group	$P\bar{1}$	*Pbca*
a / nm	0.777 6(2)	1.911 0(4)
b / nm	1.081 4(2)	0.699 0(1)
c / nm	1.291 0(3)	3.401 2(7)
α / (°)	85.28(3)	90
β / (°)	84.50(3)	90
γ / (°)	72.00(3)	90
Volume / nm^3	1.026 1(4)	4.543 6(2)
Z	2	8
D_c / ($g \cdot cm^{-3}$)	1.710	1.567
Measured reflections	10 107	38 872
Independent reflections (R_{int})	4 638 (0.032 9)	5 140 (0.109 1)
Reflection with $I \geqslant 2\sigma(I)$	3 208	4 939
F(000)	538	2304
Crystal size / mm	0.13×0.12×0.11	0.18×0.40×0.41
θ range for data collection / (°)	3.08~27.44	3.16~27.48

Continued Table 1

Number of parameters	311	333
Goodness-of-fit on F^2	1.145	1.199
a, b for weighting scheme	0.048 6, 2.081 8	0.030 0, 6.162 9
R_1, wR_2 ($I \geqslant 2\sigma(I)$)	0.045 4, 0.103 2	0.071 8, 0.124 7
R_1, wR_2 (all data)	0.084 9, 0.151 2	0.125 5, 0.147 4
$(\Delta\rho)_{max}$, $(\Delta\rho)_{min}$ / (e·nm^{-3})	692, −1 107	541, −679

[a] $R_1=\sum(|F_o|-|F_c|)/\sum|F_o|$, $wR_2=[\sum w(F_o^2-F_c^2)^2/\sum w(F_o^2)^2]^{1/2}$, and $w=[\sigma^2(F_o^2)+(aP)^2+bP]^{-1}$ where $P=(F_o^2+2F_c^2)/3$. For **1**, a= 0.030 0 and b=2.081 8. For **2**, a=0.030 0 and b=6.162 9.

Table 2 Selected bond length (nm) and angles (°) for 1 and 2

			1		
Cu-N1	0.200 2(4)	Cu-O1	0.194 7(3)	Cu-O8	0.193 6(3)
Cu-N2	0.200 0(3)	Cu-O4	0.246 7(3)		
N1-Cu-N2	82.7(1)	N2-Cu-O1	90.3(1)	O1-Cu-O8	91.9(1)
N1-Cu-O1	170.8(1)	N2-Cu-O4	90.9(1)	O4-Cu-O4	99.1(1)
N1-Cu-O4	92.1(1)	N2-Cu-O8	169.5(2)		
N1-Cu-O8	93.9(1)	O1-Cu-O4	94.0(1)		
			2		
Cu-N1	0.199 5(3)	Cu-O1	0.194 1(3)	Cu-O5	0.282 2(4)
Cu-N2	0.199 6(3)	Cu-O4	0.256 3(5)	Cu-O7	0.191 2(3)
N1-Cu-N2	81.1(1)	N2-Cu-O1	170.0(1)	O1-Cu-O5^{i}	91.6(1)
N1-Cu-O1	91.0(1)	N2-Cu-O4	87.5(1)	O1-Cu-O7	92.3(1)
N1-Cu-O4	86.2(1)	N2-Cu-O5^{i}	81.4(1)	O4-Cu-O5^{i}	164.9(1)
N1-Cu-O5^{i}	82.0(1)	N2-Cu-O7	96.6(1)	O4-Cu-O7	93.8(1)
N1-Cu-O7	177.7(1)	O1-Cu-O4	98.1(1)	O5^{i}-Cu-O7	97.6(1)

Symmetry transformations used to generate equivalent atoms: **2**: ^{i} x, y+1, z.

Table 3 Hydrogen bond lengths and bond angles for 1 and 2

D–H···A	d(D-H) / nm	d(H···A) / nm	d(D···A) / nm	∠DHA / (°)
1				
O8–H81···O2	0.097	0.161	0.254 0(5)	159.4
O8–H82···O9	0.078	0.200	0.271 0(5)	152.2
O9–H91···O3^{i}	0.083	0.206	0.289 0(6)	177.6
O9–H92···O7^{ii}	0.083	0.226	0.299 6(7)	148.3
C3–H3A···O5^{iii}	0.093	0.256	0.322 6(7)	133.4
C8–H8A···O2^{iv}	0.093	0.250	0.340 4(5)	164.4
C9–H9A···O7^{v}	0.093	0.255	0.337 6(7)	148.3
C16–H16A···O6^{v}	0.093	0.253	0.333 8(7)	145.2
2				
O7–H71···O2	0.082	0.185	0.261 6(5)	155.4
O7–H72···O4^{ii}	0.082	0.181	0.258 4(4)	157.5
C16–H16A···O3^{iii}	0.093	0.260	0.352 5(7)	175.4
C20–H20A···O5^{iv}	0.093	0.256	0.348 1(5)	173.4
C23–H23A···O5^{iv}	0.093	0.241	0.333 7(5)	176.1

Continued Table 3

C24–H24A···O2^{v}	0.093	0.232	0.324 9(6)	175.5
C26–H26A···O4^{vi}	0.093	0.241	0.330 2(5)	161.5

Symmetry transformations used to generate equivalent atoms: **1**: ^{i} $-x+2, -y, -z+1$; ^{ii} $x-1, y, z$; ^{iii} $-x+1, -y+1, -z+2$; ^{iv} $x, y+1, z$; ^{v} $-x+2, -y+1, -z+1$; 2: ^{ii} $-x+1, -y+2, -z+1$; ^{iii} $-x, y+0.5, -z+0.5$; ^{iv} $-x+1, y-0.5, -z+0.5$; ^{v} $-x+0.5, -y+1, z+1.5$; ^{vi} $x+1.5, -y+2.5, -z+1$.

2 Results and discussion

2.1 Crystal structures

2.1.1 $[Cu(phen)(H_2O)(fba)(ClO_4)]\cdot H_2O$ (**1**)

The asymmetric unit of **1** contains one Cu^{2+} ion, one phen molecule, one fba ligand, one ClO_4^- ion and two water molecules (Fig.1). Fba ion functions as monodentate ligand providing one carboxylic oxygen atom (O1) to coordinate one Cu^{2+} ion. The Cu^{2+} ion is each coordinated by two N atoms (N1, N2) of one phen molecule, three O atoms (O1, O4, O8) from one fba ligand, one ClO_4^- ion and one H_2O molecule, respectively, building up a square pyramidal CuN_2O_3 coordination environment with N1, N2, O1 and O8 atoms at the corners of the basal plane and O4 atom at the apical position. The radial Cu-N and Cu-O bond lengths fall in the range 0.193 5 (3)~0.200 1(4) nm, and the axial Cu-O bond length is 0.246 7(3) nm. The cisoid bond angles around Cu(Ⅱ) ion fall in the range 82.7(1)°~99.1(1)°, and the transoid ones are 169.5(2)° and 170.8(1)°, exhibiting significant departure from the corresponding value for a regular square pyramid (90° and 180°). The structural distortion index tau (τ) was calculated as 0.02 ($\tau=(\alpha-\beta)/60$, where α and β correspond to the two angles showing a tendency to linearity). The τ values of square-based-pyramidal and trigonal-bipyramidal extremes are 0 and 1, respectively[21]. From the above, the coordination geometry of Cu(Ⅱ) atom is one distorted square pyramid.

The complex molecules display significant intramolecular hydrogen bonds from the aqua ligand to the uncoordinating carboxylate O atoms (O2). Along [100] direction, the complex is shifted to form another one, and the lattice water molecule connects the two resulting complexes through O–H···O hydrogen bond forming 1D supramolecular single-chain. Each single-chain closes to the near one that the phen and fba ligands from different single-chains are stacked alternatively with the close interplanar distance of 0.338 and 0.341 nm, suggesting considerable $\pi\cdots\pi$ stacking interactions which contributed themselves to form double-chains (Fig.1). The resulting double-chains are further assembled into 2D layers parallel to (001) by O–H···O hydrogen bonds, and the 2D layers finally form 3D network structure via C–H···O weak hydrogen bonds.

2.1.2 $^{1}_{\infty}[Cu(bpy)(H_2O)(fba)_2]$ (**2**)

The asymmetric unit of **2** contains one Cu^{2+} ion, one bpy ligand, two crystallographically distinct fba ions and one water molecule (Fig.2). One of the fba ions functions as monodentate ligand providing one carboxylic oxygen atom (O1) to coordinate one Cu atom, while another fba ligand offers two carboxylic oxygen atoms (O4, O5) to bridge two Cu atoms. The Cu atom is coordinated by two N atoms (N1, N2) of one bpy molecule, three O atoms (O1, O4, O5^{i}, ^{i} $x, y+1, z$) from three fba ligands, respectively, and one O atom (O7) from one water molecule to form CuN_2O_4 chromophore. In the CuN_2O_4 octahedron coordination environment, N1, N2, O1 and O7 atoms locate in the corners of the basal plane and O4, O5^{i} atoms occupy the apical positions. The radial Cu-N and Cu-O bond distances fall in the range 0.191 2(3)~0.199 6(3) nm and the axial Cu-O bond lengths are 0.256 3(5) and 0.282 2(4) nm. The transoid and cisoid bond angles subtended at Cu^{2+} ion are in the range 81.1(1)°~98.1(1)° and 164.9(1)°~177.7(1)°, respectively, exhibiting significant departure from 90° and 180°. The above observation indicates that the coordination geometry is one distorted octahedron of a '4+1+1' type.

Through the O4 and O5 donors, each fba anion connectes to two Cu^{2+} cations, acting as a bridging ligand in the [010] direction to form single-chain. The

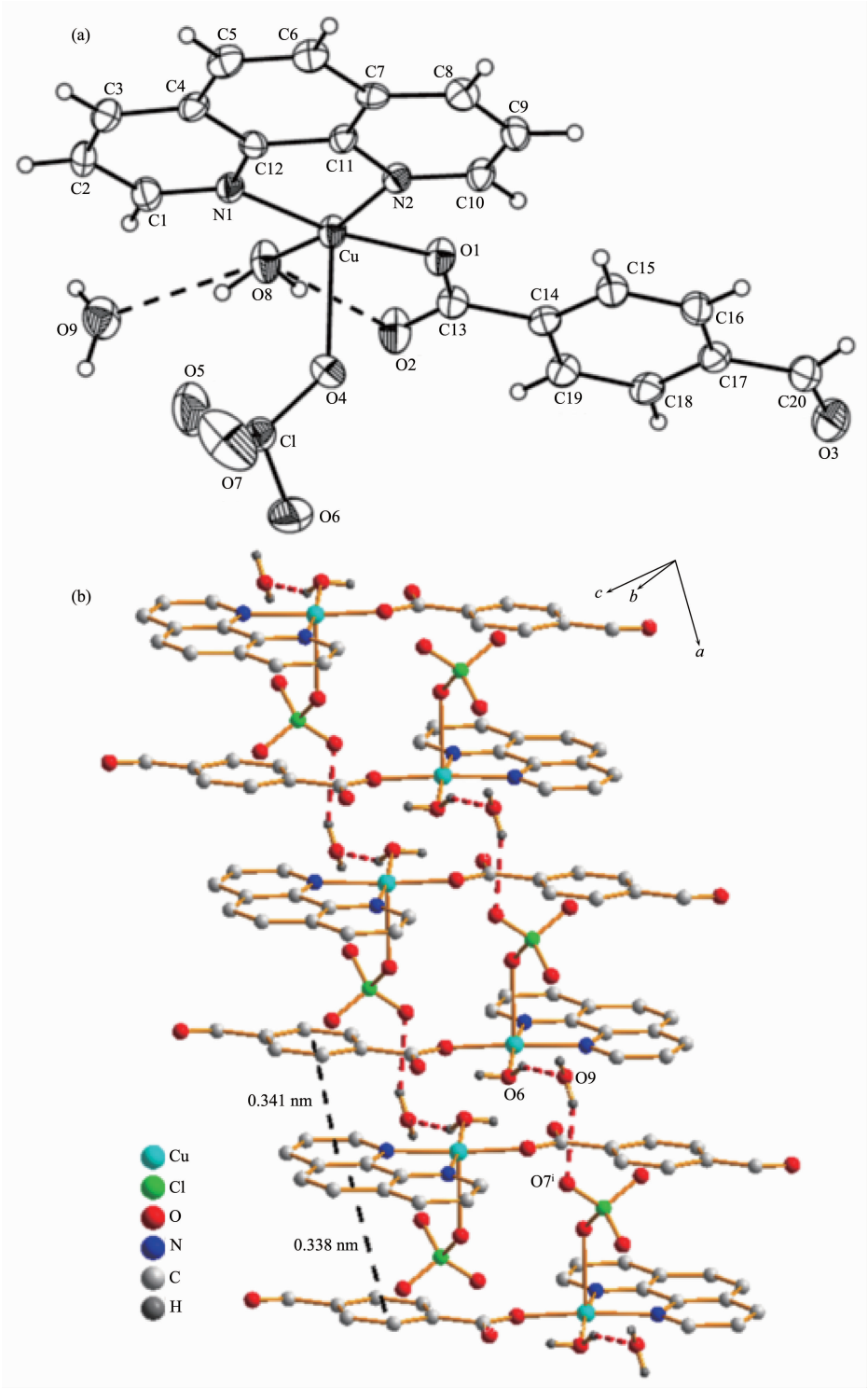

Symmetry code: ^{i} $x-1, y, z$

Fig.1 (a) ORTEP drawing with 45% probability displacement ellipsoids of complex **1**; (b) 1D double-chain in **1** sustained by O–H···O hydrogen bonds and $\pi\cdots\pi$ stacking interaction

near single-chains are close to each other leading to the formation of O–H ··· O hydrogen bonds which contributed themselves to the development of double-chains (Fig.2). The double-chains are assembled into 2D layers parallel to (001) by C–H ··· O hydrogen bonds, and the resulting 2D layers are stacked forming 3D network structure in a sequence ···AAAA ··· to meet the requirements for close-packing.

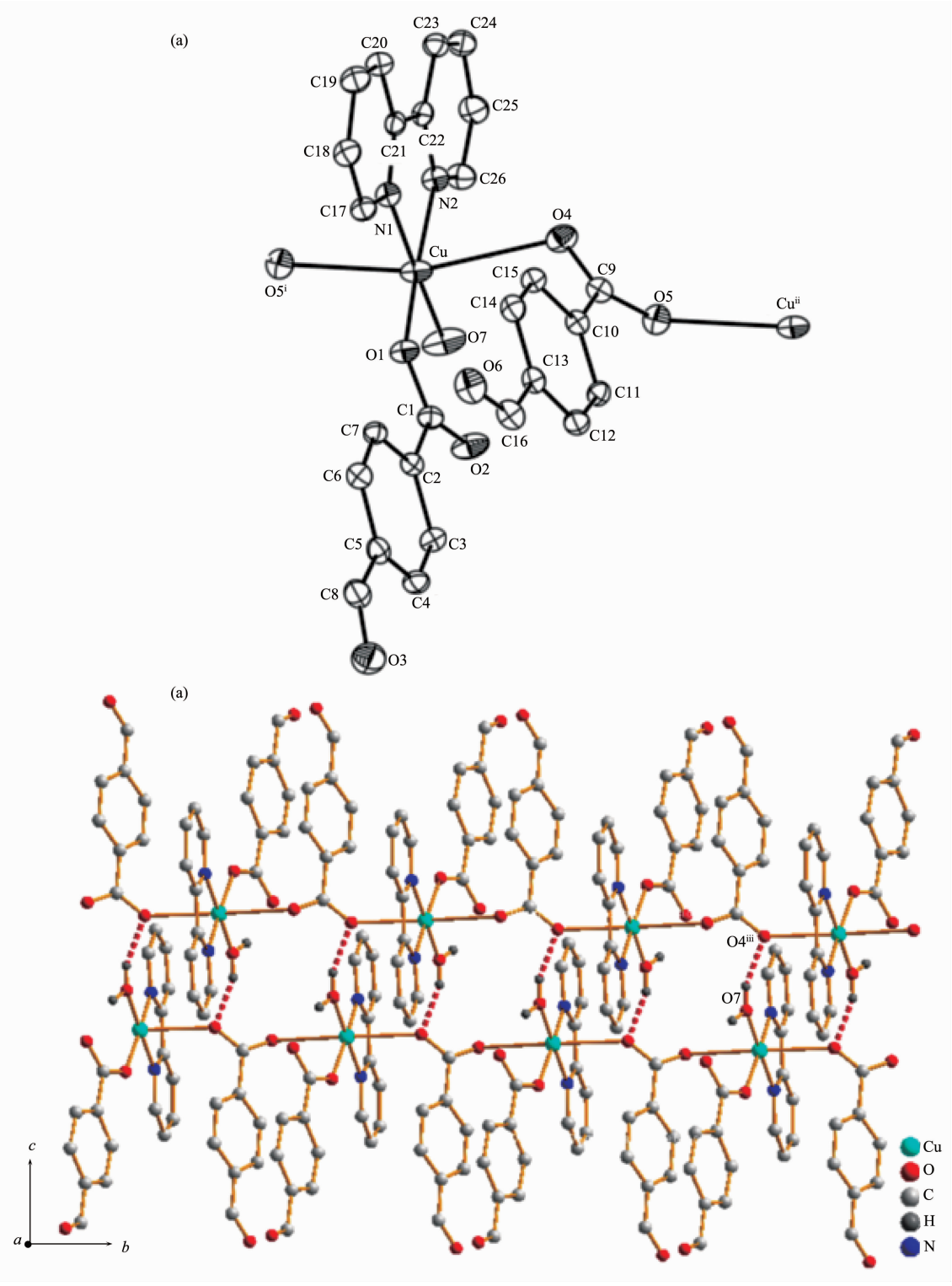

Symmetry code: [i] $x, y+1, z$; [ii] $x, y-1, z$; [iii] $-x+1, y-0.5, -z+0.5$

Fig.2　(a) ORTEP drawing with 45% probability displacement ellipsoids of complex **2**; (b) Supramolecular assemblely of **2** into 1D double-chain though O–H···O hydrogen bonds

2.2　IR spectra

IR spectrum data were described in experimental section above. The common absorptions around 3 442 cm^{-1} for **1** and 3 487 cm^{-1} for **2** approve the existence of water molecules. In both **1** and **2**, the C-H and C=O stretching of the formyl groups are observed at

2 725~2 835 and 1 696 cm^{-1}, respectively. The =C-H in-plane bending vibrations on aromatic rings emerge at 1 202~1 081 cm^{-1} for **1** and 1 203~1 032 cm^{-1} for **2**. The =C-H stretching vibrations in **1** are submerged in the large O-H absorption band of water molecule, while **2**′s appear at 3 034~3 118 cm^{-1}. The =C-H out-of-plane bending vibrations on the aromatic rings of fba at 806 and 770 cm^{-1} correspond to para-substitution in both **1** and **2**. The skeleton vibrations of C=C and C=N of aromatic rings appear at the range of 1 423~1 635 cm^{-1} in **1** and 1 451~1 558 cm^{-1} in **2**. For **1**, the typical bands of carboxylic groups appear at 1587 cm^{-1} for antisymmetric stretching (ν_{as}) and 1 398 cm^{-1} for symmetric stretching (ν_s). The value of $\Delta\nu=\nu_{as}-\nu_s=189$ cm^{-1} clearly indicates the presence of monodentate coordination mode of carboxylic groups[22]. The middle and narrow bands around 1 108 and 637 cm^{-1} of **1** correspond to the antisymmetric stretching vibration and asymmetric variable angle vibration of ClO_4^- ions. For **2**, the characteristic bands of the carboxylate groups were observed at 1 597 and 1 393 cm^{-1} for asymmetric and symmetric stretching, respectively, and the differences $\Delta\nu$=204 cm^{-1}, corresponds to the bridging mode of carboxylate groups.

2.3 Thermal analyses

The thermal stability of complexes **1** and **2** were carried out from 30 to 800 ℃ through thermogravimetric analyses (Fig.3). In both **1** and **2**, water molecules are lost at first, and complicated decomposition reactions take place upon heating. Sample **1** experiences the first weight loss of 6.3% from 70 to 140 ℃ in agreement with the removal of one coordinated and one uncoordinated water molecules (*ca.* 6.8%) and the dehydration leads to formation of an anhydrous intermediate "Cu(phen)(fba)(ClO_4)". The intermediate remains stable up to 250 ℃. When further heated, it shows a framework collapse with the removal of one phen molecule and a decomposition of intermediate "Cu(fba)(ClO_4)" simultaneously. A residue of 37.5% is collected at 800 ℃. Sample **2** experiences the initial weight loss of 3.5% in the range of 106~135 ℃ coincident with the removal of one coordinated water molecule (*ca.* 3.4%). The dehydrate intermediate Cu(bpy)$(fba)_2$ remains stable between 135 and 225 ℃. When further heated, the intermediate shows a framework collapse with the removal of phen and the decomposition of "Cu$(fba)_2$". The final residual of 24.0% was collected at 800 ℃.

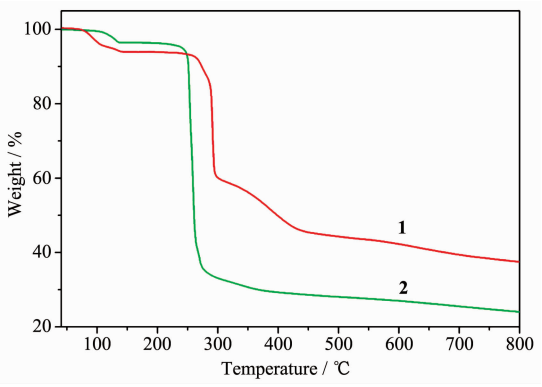

Fig.3 TG curves of **1** and **2**

2.4 Magnetic properties

The variable temperature magnetic measurements of **1** and **2** were investigated in the temperature rang of 2~300 K at an applied field of 1 000 Oe (Fig.4). For **1**, the room temperature effective magnetic moment, μ_{eff}, of 1.69μ_B is slightly lower than the spin-only value of 1.73μ_B per mole of copper(Ⅱ) (S=1/2 and g=2). The r.t. χ_mT value (0.36 $cm^3\cdot K\cdot mol^{-1}$) is very close to the spin-only value (0.37 $cm^3\cdot K\cdot mol^{-1}$). Upon cooling, the χ_mT value increases continuously to a inflection point at 40 K, and then sharply rises to a maximum value of 1.20 $cm^3\cdot K\cdot mol^{-1}$ at 7 K. Afterwards the χ_mT value witnesses an abrupt diminishing to a minimal value of 0.72 $cm^3\cdot K\cdot mol^{-1}$ at 2 K. This behavior indicates that the magnetic interactions among the Cu(Ⅱ) atoms are weak ferromagnetic and antiferromagnetic in the range of 300 to 7 K and 7 to 2 K, respectively. The χ_m obeys the Curie-Weiss law, $\chi_m=C/(T-\theta)$, with the Curie constant C=1.06 $cm^3\cdot K\cdot mol^{-1}$ and the Weiss constant θ=−0.674 K. From the viewpoint of magnetism, it is important to point out that **1** is a mononuclear structure with S=1/2 and g=2. Therefore, the experimental data of magnetic structure can be fitted to the equation Eq.**1**. Owing to the very weak magnetic interactions between ions, the expression is corrected using the molecular field approximation (Eq.**2**), to which the magnetic

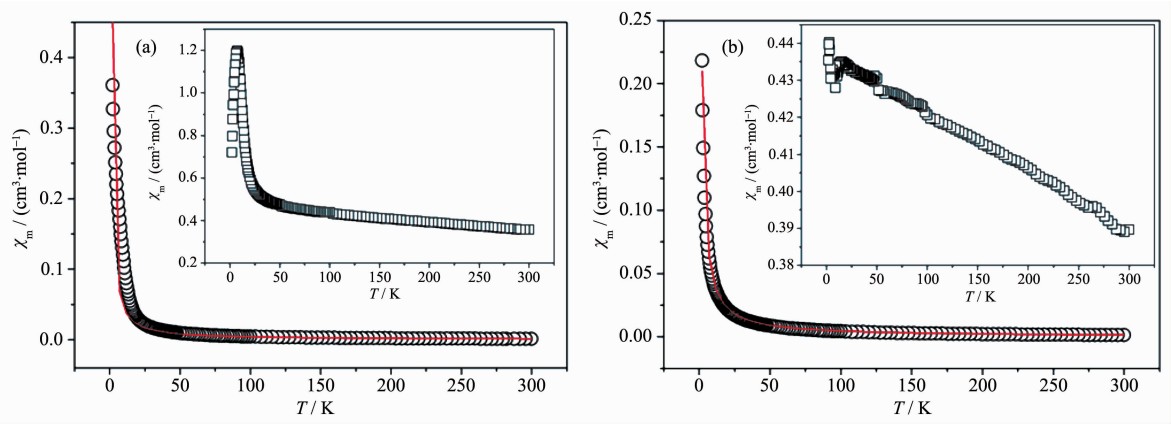

Solid lines represent the best fit

Fig.4　Temperature dependence of the magnetic susceptibility of **1** and **2**

susceptibility data were fitted.

$$\chi_m' = \frac{2N\beta^2 g^2}{3kT} S(S+1) \quad (1)$$

$$\chi_m = \frac{\chi_m'}{1-\chi_m' \cdot 2zJ'/(N\beta^2 g^2)} \quad (2)$$

Here N is Avogadro′s number, β is Bohr′s magneton, k is Boltzmann′s constant, S is the spin moment (S=1/2), and the best fit leads to g=2.087, zJ' =1.52 cm^{-1}, R=1.2×10^{-3} ($R=\sum[(\chi_m)_{obs}-(\chi_m)_{calc}]^2/[(\chi_m)_{obs}]^2$), where the positive zJ' clearly indicative the existence of ferromagnetic interactions among the Cu(Ⅱ) atoms.

For **2**, the r.t. μ_{eff} value of 1.83μ_B is somewhat larger than the spin-only value of 1.73μ_B for a ground state Cu atom. The $\chi_m T$ value (0.42 cm^3·K·mol^{-1}) at 300 K is also slightly bigger than the spin-only value (0.37 cm^3·K·mol^{-1}). Upon lowering the temperature, the $\chi_m T$ value seems to be a liner increase suggesting a weak ferromagnetic coupling between the adjacent Cu(Ⅱ) ions. The best fit of the χ_m versus T plot to the Curie-Weiss equation $\chi_m = C/(T-\theta)$ give the Curie constant C =0.430 cm^3·K·mol^{-1} and the Weiss constant θ =0.032 K indicating weak ferromagnetic interactions between the neighboring Cu (Ⅱ) ions. Taking into account that the structure is a 1D chain, the experimental data of magnetic structure can be fitted to the following equation derived by Hall[23]:

$$\chi_m = \frac{N\beta^2 g^2}{kT} \times \frac{025+0.144\ 995x+0.300\ 94x^2}{1+1.986\ 2x+0.688\ 54x^2+6.062\ 6x^3} \quad (3)$$

$$x = \frac{|J|}{kT}$$

Here the parameters have their usual meaning. The results of the fit though Eq.**3** lead to J=0.102 cm^{-1}, g=2.215, R=1.73×10^{-6} ($R=\sum[(\chi_m)_{obs}-(\chi_m)_{calc}]^2/[(\chi_m)_{obs}]^2$), in which the positive J value indicates a very weak ferromagnetic coupling between the Cu(Ⅱ) ions.

References:

[1] Dimiza F, Papadopoulos A N, Tangoulis V, et al. *J. Inorg. Biochem.*, **2012**,**107**:54-64

[2] ZHOU Hong(周宏), YU Shan-Shan(于珊珊), DUAN Hai-Bao(段海宝), et. al. *Chinese J. Inorg. Chem.* (*Wuji Huaxue Xuebao*), **2013**,**29**(7):1357-1384

[3] LI Qing-Xiang(李庆祥), XIANG Ai-Hua(向爱华), MENG Xiang-Gao(孟祥高). *Chinese J. Inorg. Chem.*(*Wuji Huaxue Xuebao*), **2013**,**29**(7):1428-1432

[4] Xu W, Liu W, Yang Y F, et al. *Inorg. Chim. Acta*, **2011**, **365**:297-301

[5] Zhou X X, Liu M S, Lin X M, et al. *Inorg. Chim. Acta*, **2009**,**362**:1441-1447

[6] Dimiza F, Papadopoulos A N, Tangoulis V, et al. *J. Inorg. Biochem.*, **2012**,**107**:54-64

[7] KUANG Yun-Fei(邝云飞), LI Chang-Hong(李昶红), LI Wei(李薇), et al. *Chinese. J. Struct. Chem.* (*Jiegou Huaxue*), **2007**,**26**(7):749-752

[8] Hou G G, Ma J P, Wang L, et al. *CrystEngComm*, **2010**,**12**: 4287-4303

[9] Jian F F, Wang Z X, Bai Z P, et al. *Transition Met. Chem.*, **1999**,**24**(5):589-594

[10]Baca S G, Simonov Y A, Gdaniec M, et al. *Inorg. Chem. Commun.*, **2003**,**6**:685-689

[11]Sertcelik M, Tercan B, Sahin E, et al. *Acta Cryst.*, **2009**, **E65**:m326-m327

[12]Deng Z P, Gao S, Ng S W. *Acta Cryst.*, **2006**,**E62**:m2904-m2905

[13]Deng Z P, Gao S, Huo L H, et al. *Acta Cryst.*, **2007**,**E63**:m2818

[14]Dimiza F, Perdih F, Tangoulis V, et al. *J. Inorg. Biochem.*, **2011**,**105**:476-489

[15]Moncol J, Jomova K, Porubska M. *Acta Cryst.*, **2012**,**C68**:m85-m89

[16]LI Wei(李薇), LI Chang-Hong(李昶红), YANG Ying-Qun(杨颖群), et al. *Chinese J. Inorg. Chem.*(*Wuji Huaxue Xuebao*), **2006**,**22**(1):101-105

[17]Qi J L, Xu W. *Acta Cryst.*, **2012**,**E68**:m1062-m1063

[18]Qi J L, Xu W, Zheng Y Q. *Z. Naturforsch.*, **2012**,**67b**:1185-1190

[19]Sheldrick G M. *SHELXS*-97, *Program for the Solution of Crystal Structure*, Germany: University of Göttingen, **1997**.

[20]Sheldrick G M. *SHELXL*-97, *Program for the Refinement of Crystal Structure*, Germany: University of Göttingen, **1997**.

[21]Addison A W, Rao N. *J. Chem. Soc., Dalton Trans.*, **1984**:1349-1356

[22]Nakamoto K. *Infrared and Rama Spectra of Inorganic and Coordination Compounds*. *4th Ed.* New York: Wiley, **1986**.

[23]Hall J W. *Theses for the Doctorate of University of North Carolina.* **1977**.